Supplementary File 1

Strategic redesign of the central metabolism in *Pseudomonas putida* for boosted NADPH generation and product formation

Maria Martin-Pascual[1,5], Stijn Kral[1], Adrian Garcia-Martinez[1], Foppe van der Meulen[1], Lissane Temming[1], Jordy Mullink[1], Lyon Bruinsma[1,5], Sara Moreno-Paz[1], Christos Batianis[1,5], Enrique Asin-Garcia[1,5], Luis Garcia-Morales[1], Markus Jeschek[6], Vitor A. P. Martins dos Santos[4,5,*], Richard van Kranenburg[2,3,*]

[1] Laboratory of Systems and Synthetic Biology, Wageningen University & Research, Wageningen, 6708 WE, The Netherlands

[2] Corbion, Gorinchem, 4206 AC, The Netherlands

[3] Laboratory of Microbiology, Wageningen University & Research, Wageningen, 6708 WE, The Netherlands

[4] LifeGlimmer GmbH, Berlin, 12163, Germany

[5] Bioprocess Engineering Group, Wageningen University & Research, Wageningen, 6700 AA, The Netherlands

[6] Department of Biosystems Science and Engineering, ETH Zurich, Basel, Zwitzerland

* Shared corresponding authors. Richard van Kranenburg; Email: richard.van.kranenburg@corbion.com & Vitor A. P. Martins dos Santos; Tel: +31317482865; Email: vitor.martinsdossantos@wur.nl

Growth curves of *P. putida* WT, *P. putida* Δ*gcd*Δ*edd* and *P. putida* Δ*gcd*Δ*edd*Δ*hexR*

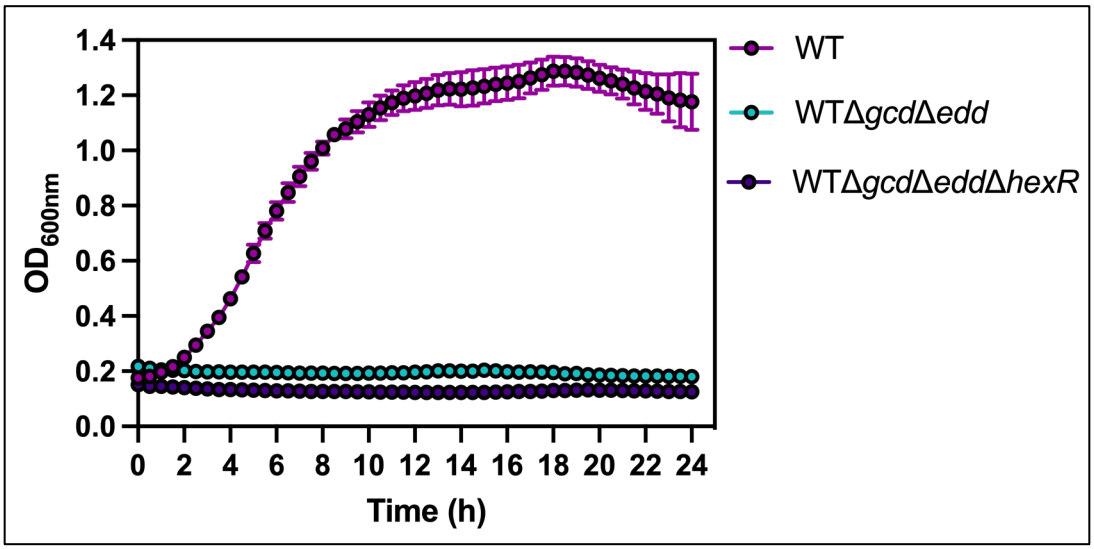

Figure S1. Growth curves of *P. putida* WT, WTΔ*gcd*Δ*edd* and WTΔ*gcd*Δ*edd*Δ*hexR*. The OD of the strains grown on M9 minimal media supplemented with 70 mM of glucose was measured over 24 hours, at a wavelength of 600 nm (OD_{600nm}) in a microplate reader. Values represent the mean and standard deviation of three biological replicates.

Growth curves of *P. putida* WT, *P. putida* Δ*gcd*Δ*edd* and *P. putida* Δ*gcd*Δ*edd*Δ*hexR* with different plasmids

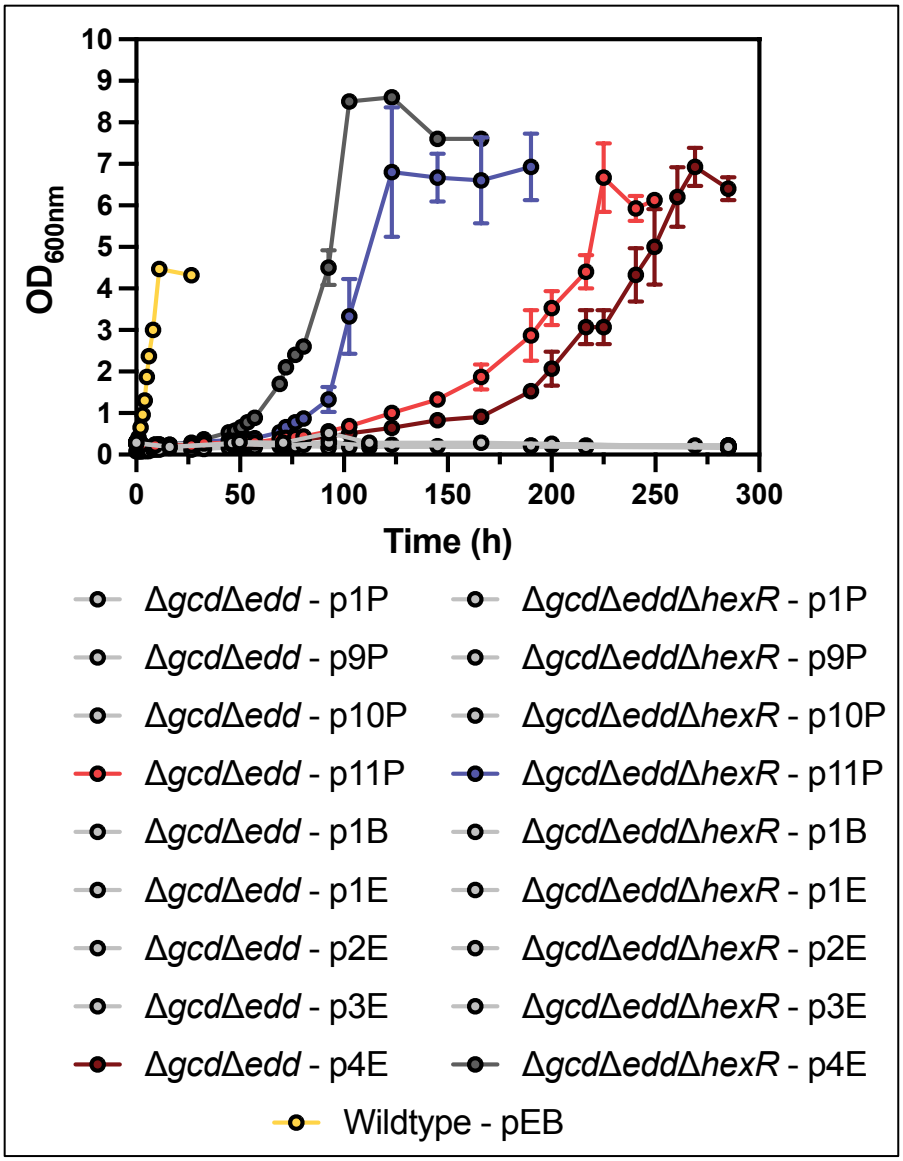

Figure S2. Growth curves of *P. putida* WT, WTΔ*gcd*Δ*edd* and WTΔ*gcd*Δ*edd*Δ*hexR* with different plasmids. The OD of the strains grown on M9 minimal media supplemented with 70 mM of glucose was measured over 285 hours, at a wavelength of 600 nm (OD_{600nm}) in a microplate reader. Values represent the mean and standard deviation of three biological replicates.

Correlating the OD_{600nm} with the cell dry weight

The cell dry weight (CDW) of *P. putida* WT and WTΔ*gcd*Δ*edd*Δ*hexR*_p7P was determined. A linear correlation through the data points shows that the relation between the OD_{600nm} and CDW for *P. putida* WT is 1: 0.52 ± 0.007 and for WTΔ*gcd*Δ*edd*Δ*hexR*_p7P is 1: 0.53 ± 0.015, which are in line with the values obtained in previous experiments[1]. WTΔ*gcd*Δ*edd*Δ*hexR*_p7P reaches higher OD_{600nm} values than *P. putida* WT. This study shows that the increased OD_{600nm} is due to increased cell mass, as *P. putida* WT and WTΔ*gcd*Δ*edd*Δ*hexR*_p7P show no significant difference in their relationship between the CDW and the OD_{600nm}. WTΔ*gcd*Δ*edd*Δ*hexR*_p7P produces more biomass than *P. putida* WT in the same media and under the same starting conditions.

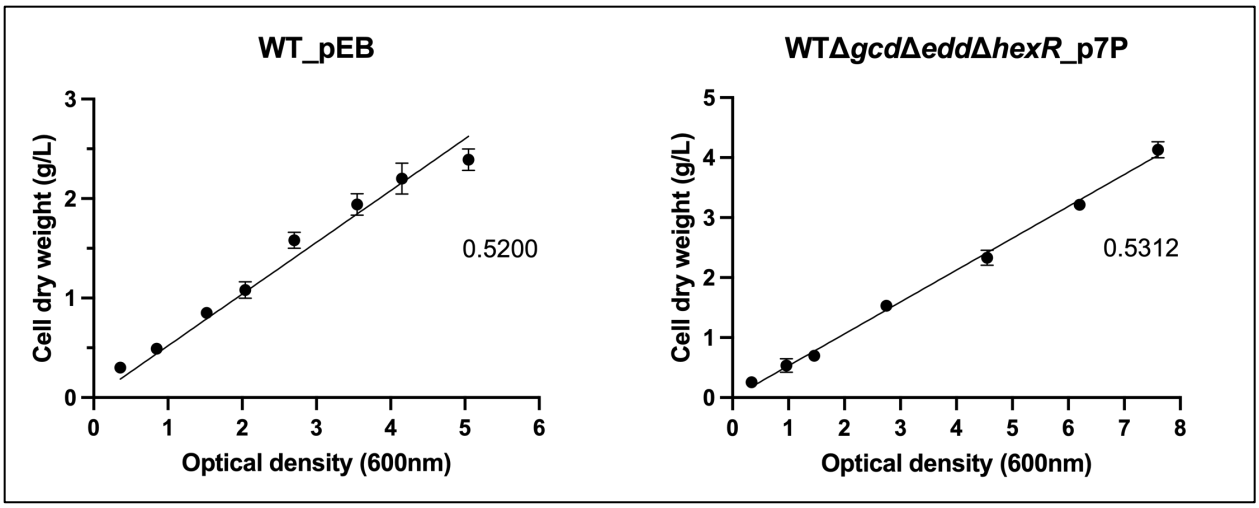

Figure S3. Correlating the Cell dry weight (CDW) to the OD_{600nm} in WT_pEB and WTΔ*gcd*Δ*edd*Δ*hexR*_p7P. The cell dry weight (g/L) of cultures was measured at different cell densities (OD_{600nm}) for WT_pEB and WTΔ*gcd*Δ*edd*Δ*hexR*_p7P. Values represent the mean and standard deviation of three replicates.

Characterizing the growth of WTΔ*gcd*Δ*edd*Δ*hexR* strains in small 1-L bioreactors

A growth experiment with WT_pEB, WTΔ*gcd*Δ*edd*Δ*hexR*_p4E and WTΔ*gcd*Δ*edd*Δ*hexR*_p7P in 1L-bioreactors was performed. The specific growth rate, maximum OD_{600nm} value and biomass yield were determined (**Table S1**). The doubling time of WT_pEB, WTΔ*gcd*Δ*edd*Δ*hexR*_p4E and WTΔ*gcd*Δ*edd*Δ*hexR*_p7P; 9.11 h ± 0.24, 13.0 8 h and 0.97 h ± 0.04 respectively, was lower than in the shake flask experiment being 15.2 h ± 0.92, 24.75 h and 2.0 h ± 0.12, respectively (**Table S1**). The maximal cell density reached was significantly higher for both mutant strains than WT_pEB, consistent with previous growth experiments. Additionally, the yield of biomass on glucose ($Y_{X/S}$) was determined (**Table S1**). The $Y_{X/S}$ value of WT_pEB ranged from 0.4 to 0.5 gCDW·g-1, corresponding to literature values of 0.47 gCDW·g-1 ± 0.05[2]. The $Y_{X/S}$ value of WTΔ*gcd*Δ*edd*Δ*hexR*_p4E was 0.43 gCDW·g-1and the $Y_{X/S}$ value of WTΔ*gcd*Δ*edd*Δ*hexR*_p7P was 0.35 gCDW·g-1. These growth rates and $Y_{X/S}$ values can be related with the metabolic flux of the strains. The lower growth rates and $Y_{X/S}$ values of WTΔ*gcd*Δ*edd*Δ*hexR*_p7P was due to the higher carbon loss at the 6-phosphogluconate (6PG) to ribulose-5-phosphate (Ri5P) the reaction compared with the *P. putida* WT. WTΔ*gcd*Δ*edd*Δ*hexR*_p4E reduces the carbon loss at the node where the 6PG is converted into Ri5P by enabling the conversion from xylulose-5-phosphate (X5P) to glyceraldehyde-3-phosphate (G3P) and acetyl-phosphate (Acp), which can be directly degraded to acetyl-CoA. By reducing this carbon loss, the growth rate, and $Y_{X/S}$ values of WTΔ*gcd*Δ*edd*Δ*hexR*_p4E are higher than WTΔ*gcd*Δ*edd*Δ*hexR*_p7P.

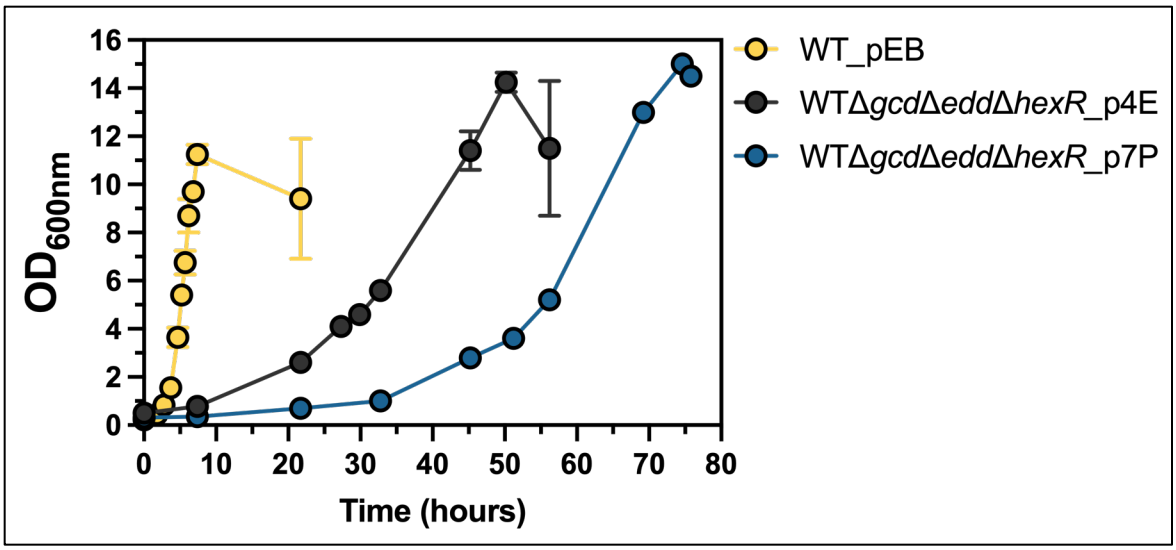

Figure S4. Growth curves of WT_pEB, WTΔ*gcd*Δ*edd*Δ*hexR*_p4E and WTΔ*gcd*Δ*edd*Δ*hexR*_p7P. Strains were grown in 1L tabletop bioreactors containing 500 mL of M9 media with 100 mM glucose. Each point is the average of two duplicate reactors, except for WTΔ*gcd*Δ*edd*Δ*hexR*_p7P, which is based on only one reactor. The optical density was measured over 72 hours, at a wavelength of 600 nm (OD_{600nm}).

Cell Preparation and Fluorescence Measurements

Overnight cultures were centrifuged at 4,000 rpm and 4°C for 8 minutes. Following centrifugation, the cell pellet was washed twice with Phosphate-Buffered Saline (PBS) and subsequently resuspended in PBS to an optical density at 600 nm (OD_{600nm}) of 1.0. The cell suspension was then transferred to a 96-well black plate with clear bottoms. For cell permeabilization, 0.05% (w/v) CTAB (final concentration) was added, followed by a brief incubation at room temperature for 2 minutes. Different NADPH concentrations, ranging from 0.01 to 1 mM, were introduced to the CTAB-treated cells. The optical density and fluorescence of the samples were measured in a microplate reader (Synergy™ Mx by BioTek) using 96 wells plates in a total volume of 200 µL per well. The optical density was determined at 600 nm, while fluorescence readings were taken with an excitation wavelength of 395 nm and an emission wavelength of 451 nm. Based on the data acquired, a calibration curve correlating NADPH concentration to fluorescence intensity was constructed (**Figure S4**).

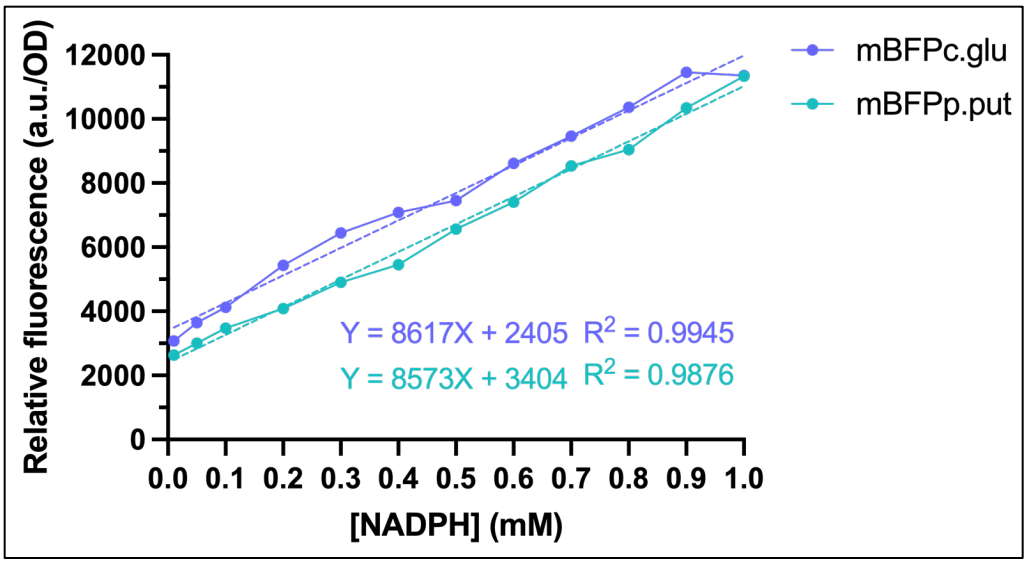

Figure S5. Calibration curve of NADPH concentrations against relative fluorescence intensity. Relative fluorescence intensities were plotted against different amounts of added NADPH concentrations to CTAB permeabilized *P. putida* cells. The NADPH-dependent blue fluorescent protein (mBFP) was used as biosensor (λ(ex) = 380 nm, λ(em) = 451 nm). The teal line represents data for mBFP codon optimized for *P. putida* (relationship given by Y = 8617X + 2405 with R^2 = 0.9945), while the purple line indicates mBFP codon optimized for *C. glutamicum* (relationship given by Y = 8573X + 3404 with R^2 = 0.9876). Each dot represents an individual *in vivo* fluorescence measurement divided the OD of the cells, which was measured at a wavelength of 600 nm.

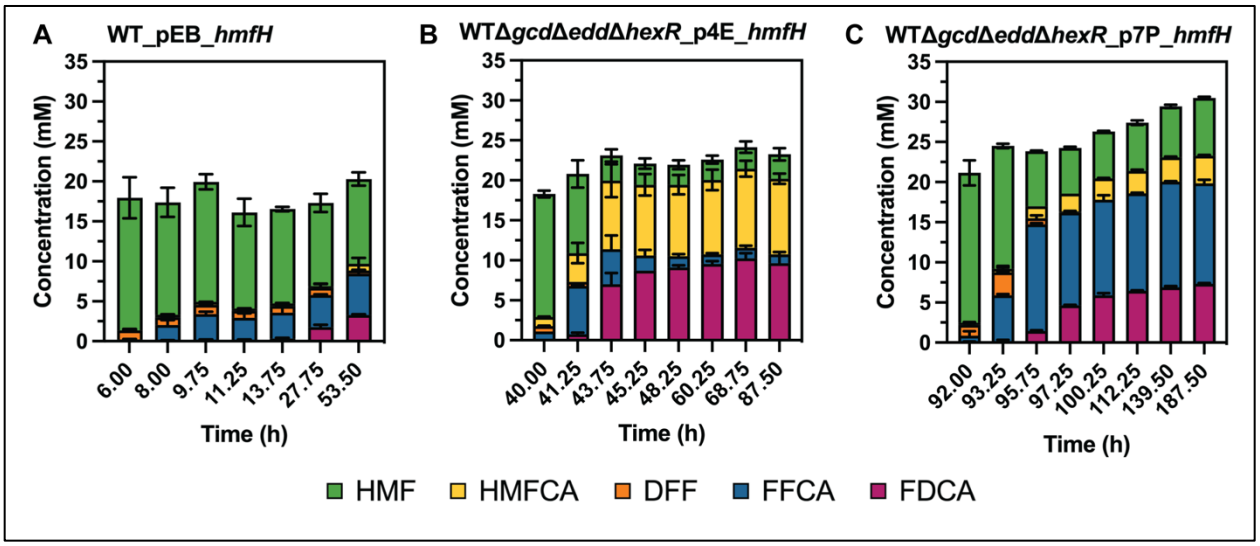

Figure S6. FDCA production in 250 mL-shake flasks with 25 mL of M9 minimal media supplemented with glucose. Graphical representation of the HMF conversion into FDCA and other reaction intermediates (HMFCA, DFF, and FFCA) by **A)** WT_pEB_*hmfH*, **B)** WTΔ*gcd*Δ*edd*Δ*hexR*_p4E_*hmfH* and **C)** WTΔ*gcd*Δ*edd*Δ*hexR*_p7P_*hmfH*. The bars represent the average of three technical replicates, and error bars represent the standard deviation. Compounds in this figure are abbreviated as follows: 5-hydroxymethylfurfural (HMF), 5-hydroxymethyl-2-furancarboxylic acid (HMFCA), 2,5-diformylfuran (DFF), 5-formyl-2-furancarboxylic acid (FFCA), and 2,5-furandicarboxylic acid (FDCA).

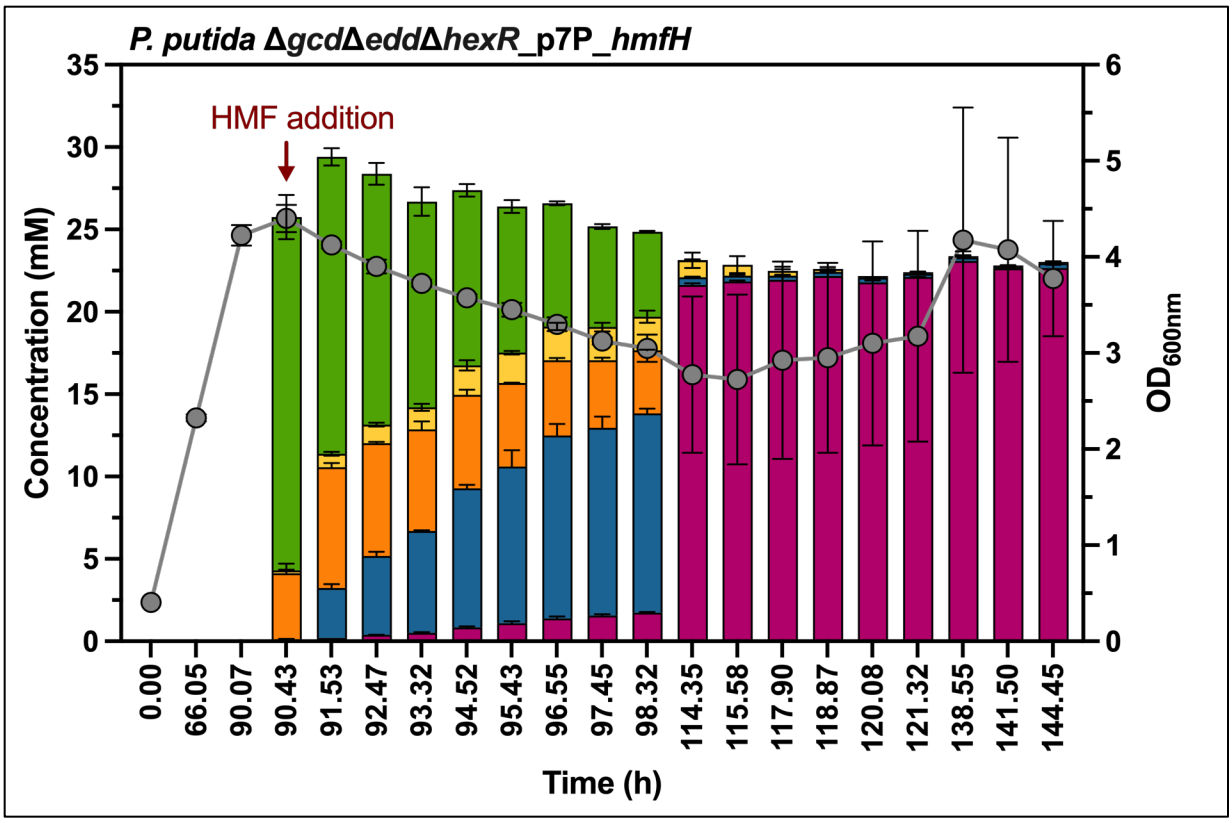

Figure S7. FDCA production of WTΔ*gcd*Δ*edd*Δ*hexR*_p7_*hmfH* in 1-L bioreactors. Graphical representation of the growth and HMF conversion into FDCA and other reaction intermediates (HMFCA, DFF, and FFCA) by WTΔ*gcd*Δ*edd*Δ*hexR*_p7P_*hmfH*. The red arrow represents the addition of 25 mM HMF. Data points (OD_{600nm}) and bars (HMF, HMFCA, DFF, FFCA, and FDCA concentrations) represent the average of two technical replicates, and error bars represent the standard deviation. Compounds in this figure are abbreviated as follows: 5-hydroxymethylfurfural (HMF), 5-hydroxymethyl-2-furancarboxylic acid (HMFCA), 2,5-diformylfuran (DFF), 5-formyl-2-furancarboxylic acid (FFCA), and 2,5-furandicarboxylic acid (FDCA).

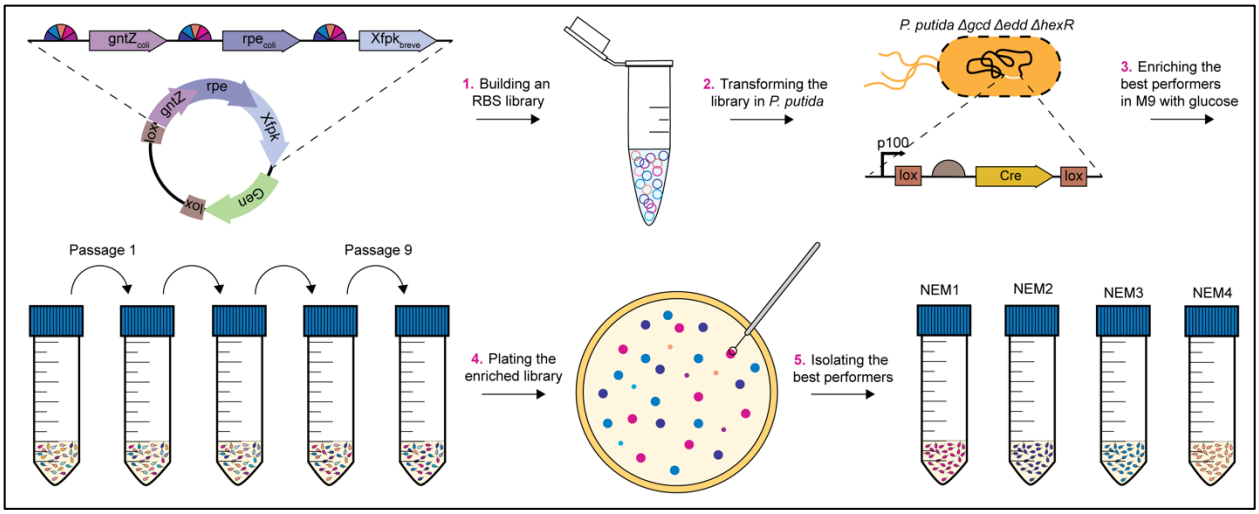

Figure S8. Workflow to build a library of RBS sequences for *gntZ*, *rpe* and *xfpk* genes using the CRE-like recombination method[3]. Step 1: we first amplified each gene using forward primers that included a Ribosome Binding Site (RBS) with degenerative nucleotides, creating a library of the gntZ-rpe-xfpk genes.

All genes and a non-replicative backbone were ligated using Golden Gate. As result, an operon library with *gntZ-rpe-xfpk* genes carrying all precicted RBS combinations was constructed. Step 2: The library was electroporated in *P. putida* Δ*gcd*Δ*edd*Δ*hexR* with a Cre-*lox* cassette integrated into its genome. The Cre-*lox* cassette comprised the *cre* gene flanked by two *lox* sites (*lox*71 and *lox*2/66), with a constitutive promoter BBa_J23100 upstream of *lox*71 and a T7 transcriptional terminator downstream of *lox*2/66. Step 3: *P. putida* Δ*gcd*Δ*edd*Δ*hexR* with the *gntZ-rpe-xfpk* operon library was grown in 50-mL falcon tubes, containing 10 mL M9 minimal media supplemented with 70 mM of glucose and gentamycin. A total of 10 passages were performed. Step 4: The liquid culture from passage 10 was plated in agar M9 minimal media supplemented with 70 mM of glucose and gentamycin to isolate individual colonies. Step 5: The largest colonies were selected and grown in 50-mL falcon tubes, containing 10 mL M9 minimal media supplemented with 70 mM of glucose and gentamycin.

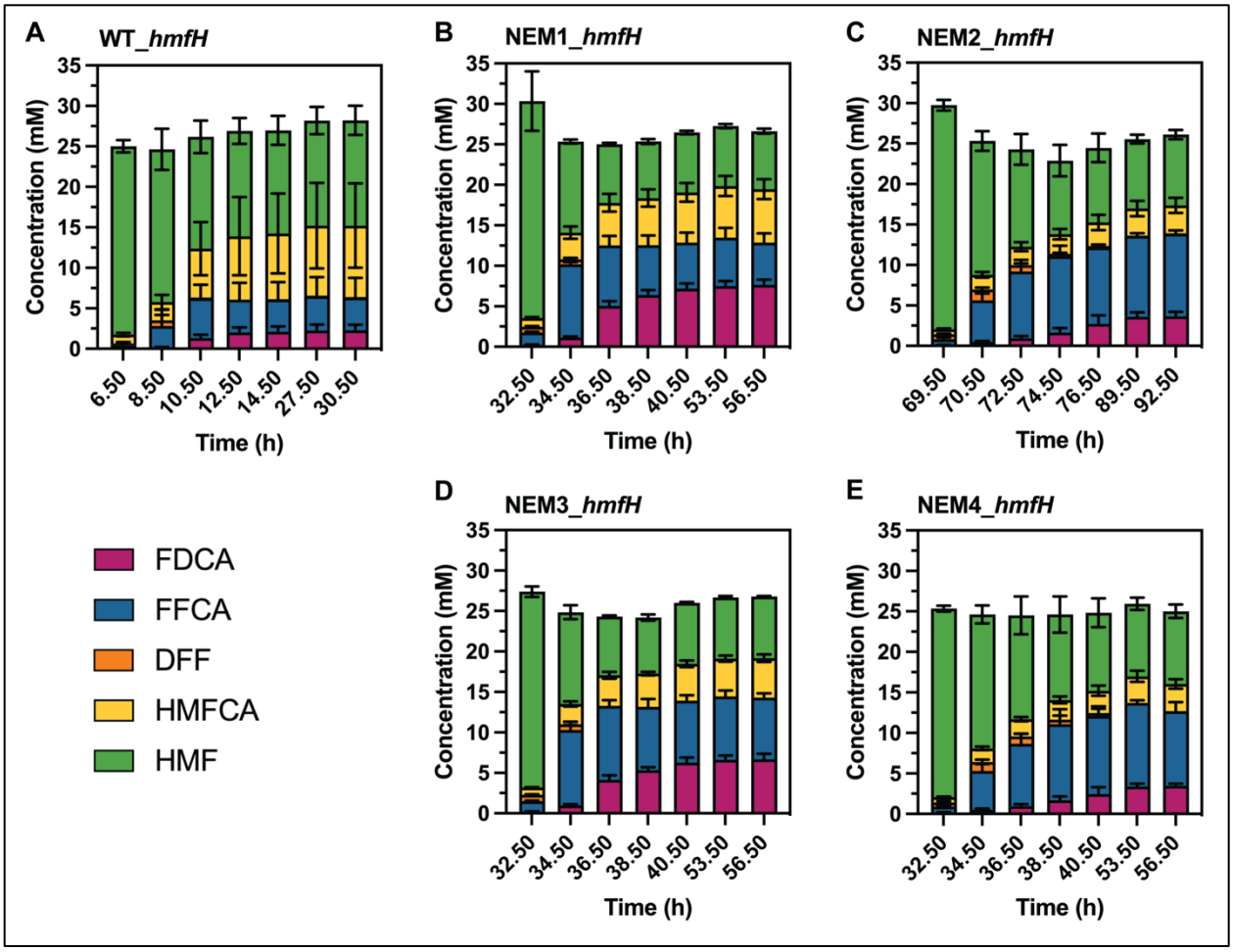

Figure S9. FDCA production in 250 mL-shake flasks with 25 mL of M9 minimal media supplemented with glucose. Graphical representation of the HMF conversion into FDCA and other reaction intermediates (HMFCA, DFF, and FFCA) by **A)** WT_*hmfH*, **B)** NEM1_*hmfH*, **C)** NEM2_*hmfH*, **D)** NEM3_*hmfH* and **E)** NEM4_*hmfH*. The bars represent the average of three technical replicates, and error bars represent the standard deviation. Compounds in this figure are abbreviated as follows: 5-hydroxymethylfurfural (HMF), 5-hydroxymethyl-2-furancarboxylic acid (HMFCA), 2,5-diformylfuran (DFF), 5-formyl-2-furancarboxylic acid (FFCA), and 2,5-furandicarboxylic acid (FDCA).

Table S1. Growth characterization of *P. putida* Δ*gcd*Δ*edd* and *P. putida* Δ*gcd*Δ*edd*Δ*hexR* strains

Strain	μ (h^{-1})	Doubling time (h)	Max OD_{600nm}	$Y_{X/S}$ ($g_{CDW} \cdot g_{glucose}$)	Experiment
WT_pEB	0.3233	2.17 (±0.04)	5 (±0.4)	-	Figure 1C (Flask)
WTΔ*gcd*Δ*edd*Δ*hexR*_p4E	0.0619	11.19 (±0.24)	7 (±0.4)	-	Figure 1C (Flask)
WTΔ*gcd*Δ*edd*Δ*hexR*_p7P	0.0286	24.75 (±0.80)	6.8 (±0.12)	-	Figure 1C (Flask)
WT_pEB	0.348	2 (±0.12)	4.47 (±0.12)	0.56 (±0.12)	Figure 1F (Flask)
*Δgcd*Δ*edd* – p4E	0.019	36.7 (±0.98)	6.93 (±0.46)	0.34 (±0.04)	Figure 1F (Flask)
*Δgcd*Δ*edd* – p11P	0.015	45.9 (±1.43)	6.67 (±0.83)	0.32 (±0.04)	Figure 1F (Flask)
*Δgcd*Δ*edd*Δ*hexR* – p4E	0.045	15.6 (±0.44)	8.6 (±0.14)	0.50 (±0.10)	Figure 1F (Flask)
*Δgcd*Δ*edd*Δ*hexR* – p11P	0.046	15.2 (±0.92)	6.93 (±0.81)	0.39 (±0.02)	Figure 1F (Flask)
WT_pEB	0.71	0.97 (±0.04)	11.5	0.48	Figure S3 (Bioreactor)
WTΔ*gcd*Δ*edd*Δ*hexR*_p4E	0.076	9.11 (±0.24)	14	0.43	Figure S3 (Bioreactor)
WTΔ*gcd*Δ*edd*Δ*hexR*_p7P	0.053	13.08	13	0.35	Figure S3 (Bioreactor)
WTΔ*gcd*Δ*edd*Δ*hexR*_p4E	0.05 (±0.001)	13.79 (±0.15)	7.27 (±0.31)	0.49 (±0.03)	Figure 5C (Flask)
NEM1	0.07 (±0.007)	9.53 (±0.90)	6.47 (±0.12)	0.59 (±0.08)	Figure 5C (Flask)
NEM2	0.04 (±0.003)	16.38 (±1.34)	6.27 (±0.46)	0.41 (±0.06)	Figure 5C (Flask)
NEM3	0.07 (±0.005)	9.65 (±0.65)	6.07 (±0.46)	0.52 (±0.05)	Figure 5C (Flask)
NEM4	0.08 (±0.002)	9.18 (±0.27)	5.47 (±0.42)	0.47 (±0.06)	Figure 5C (Flask)

Table S2. NADPH analysis in the engineered *P. putida* strains using mBFP *in vivo* sensor

	OD range	*P. putida_ Ctrl_mBFP*	SD	*P. putida Δgcd Δedd Δ hexR_p7P_ mBFP*	SD	*P. putida Δgcd Δedd Δ hexR_p4E_ mBFP*	SD
Lag phase	0.10-0.14	41200	1456.907	222000	38560	276000	10481.76
	0.24-0.32	42900	621.2807	659000	59396	376000	3717.221
Early exponential phase	0.44-0.47	43800	2785.087	572000	130053.1	382000	5201.577
	0.57-0.60	47400	1873.005	575000	161336.4	392000	2669.375
Late exponential phase	0.76-0.79	50600	1961.916	460000	158311.2	373000	21615
	0.90-1.00	59400	2044.19	379000	151980.2	378000	5835.139
	1.38-1.42	52700	1414.368	326000	90265.16	359000	9986.045
Stationary phase	1.52-1.60	60500	6939.505	310000	36855.4	343000	7257.685

Table S2. Growth rate and doubling time of *P. putida* strains containing one or more active GAPDH enzymes.

Strain	Active GAPHD	μ (h^{-1})	Doubling time (h^{-1})	Experiment
Wild type	GAPA, GAPB, PP_3443 and PP_0665	0.43 ±0.04	1.62 ±0.12	Figure 3B
ΔPP_3443ΔPP_0665	GAPA and GAPB	0.36 ±0.02	1.92 ±0.09	Figure 3B
ΔgapAΔgapB	PP_3443 and PP_0665	0.38 ±0.05	1.82 ±0.12	Figure 3B
ΔPP_3443ΔPP_0665ΔgapB	GAPA	0.41 ±0.04	1.70 ±0.10	Figure 3B
ΔPP_3443ΔPP_0665ΔgapA	GAPB	0.12 ±0.02	5.98 ±0.21	Figure 3B
ΔgapAΔgapBΔPP_0665	PP_3443	0.38 ±0.03	1.81 ±0.08	Figure 3B
ΔgapAΔgapBΔPP_3443	PP_0665	0.14 ±0.01	4.86 ±0.17	Figure 3B

Table S3: Overview of the gene composition of the plasmids. All plasmids have a pSEVAb23 backbone.

Plasmid name	Genes	Organism
p1P	*gntZ*	*P. putida* KT2440
p2P	*zwf-1*	*P. putida* KT2440
p3P	*glk–pgl–gntZ*	*P. putida* KT2440
p4P	*glk–pgl–gntZ–gapA–gapB*	*P. putida* KT2440
p5P	*gapA–gapB*	*P. putida* KT2440
p6P	*tal–gapA–gapB*	*P. putida* KT2440

p7P	*tktA–tal–gapA–gapB*	*P. putida* KT2440
p8P	*rpe–tktA–tal*	*P. putida* KT2440
p9P	*rpe*	*P. putida* KT2440
p10P	*gntZ–rpe*	*P. putida* KT2440
p11P	*gntZ–rpe–xfpk*	*P. putida* and *B. breve*
p1B	*xfpk*	*B. breve*
p1E	*gntZ*	*E. coli*
p2E	*rpe*	*E. coli*
p3E	*gntZ–rpe*	*E. coli*
p4E	*gntZ–rpe–xfpk*	*E. coli* and *B. breve*
pSEVAb62-mBFP	*mBFP*	*Codon optimized for P. putida*
pSEVAb62-pTAC-*hmfH*	*hmfH*	*Cupriavidus basilensis* HMF14
pSEVAb62-p100-*vioABCDE*	*vioABCDE*	*Chromobacterium violaceum*

Table S4. RBS sequence variants. RBS sequences present in the most optimal strains obtained from the RBS library. The corresponding translation initiation rate of each RBS was predicted using the RBS calculator tool by Salis et al. (2009)[4].

Strain	Gene	Sequence	Predicted translation initiation rate
NEM1	*gntZ*	AATTTGAGGAGGAATTA	791.72
	rpe	ATATGAGGATGAATATA	42.11
	xfpk	TTAAGTGAGGCATTAAT	111.26
NEM2	*gntZ*	AATTTAAGGAGGAATTA	1576.2
	rpe	ATATAAGGAGGAATATA	646.81
	xfpk	TTAAGTAAGGTATTAAT	160.3
NEM3	*gntZ*	AATTTGAGGAGGAATTA	791.72
	rpe	ATATTAGGAGGAATATA	314.81
	xfpk	TTAAGTAAGGCATTAAT	118.57
NEM4	*gntZ*	AATTTGAGGGGGAATTA	350.59
	rpe	ATATGAGGAACCATATA	22.33
	xfpk	TTAAGGGAGGAATTAT	597.85
WTΔ*gcd*Δ*edd*Δ*hexR*_p4E	*gntZ*	AAAGAGGAGAAA	84.36
	rpe	AAAGAGGAGAAA	16.25
	xfpk	AAAGAGGAGAAA	156.28

Data analysis S1

Growth rates (μ) were calculated by plotting the OD_{600nm} data in a logarithmic scale. Next, the trendline of the exponential phase was added to obtain the equation of the curve in the form of $y=Ae^{Bx}$, where x is equal to μ.

Equation 1: $Doubling\ time = \frac{Ln(2)}{\mu}\ [h]$

Equation 2: $CDW_{(t)} = OD_{600(t)} * ODCDW\ factor\ [g_{DCW} * L^{-1}]$

Equation 3: $Y_{\frac{X}{S}} = \frac{CDW_{(max)}}{Glucose\ concentration_{initial} - Glucose\ concentration_{final}}\ \left[g_{DCW} * {g_{glucose}}^{-1}\right]$

Equation 4: $FDCA_{Produced(t)} = FDCA_{(t)} - FDCA_{(t-1)}\ [mM]$

Equation 5: $HMF_{conversion} = \frac{HMF_{initial} - HMF_{final}}{HMF_{initial}} * 100\ [\%]$

Equation 6: $q_{FDCA(t)} = \frac{FDCA_{Produced(t)}}{CDW_{(t)} * time}$ $[\mu mol_{FDCA} * {g_{DCW}}^{-1} * h^{-1}]$

Equation 7: $Q_{FDCA(t)} = q_{FDCA(t)} * CDW_{(t)}$ $[\mu mol_{FDCA} * L^{-1} * h^{-1}]$

Equation 8: $FDCA_{Produced,total} = FDCA_{final} - FDCA_{initial}$ $[g_{FDCA}]$

Equation 9: $HMF_{Converted,total} = HMF_{initial} - HMF_{final}$ $[g_{HMF}]$

Equation 10: $Y_{FDCA/HMF} = \frac{FDCA_{Produced,total}}{HMF_{Converted,total}}$ $[g_{FDCA} * {g_{HMF}}^{-1}]$

REFERENCES

1. Kuepper, J. *et al.* Metabolic Engineering of Pseudomonas putida KT2440 to Produce Anthranilate from Glucose. *Frontiers in Microbiology* **6**, (2015).
2. Martínez-García, E., Nikel, P. I., Aparicio, T. & de Lorenzo, V. Pseudomonas 2.0: genetic upgrading of P. putida KT2440 as an enhanced host for heterologous gene expression. *Microbial Cell Factories* **13**, 159 (2014).
3. Batianis, C. Tailoring Pseudomonas putida for industrial biocatalysis. (2022) doi:10.18174/561955.
4. Salis, H. M., Mirsky, E. A., & Voigt, C. A. Automated design of synthetic ribosome binding sites to control protein expression. *Nature Biotechnology* **27**, 946-950 (2009).